

GNSS Offline Signal Quality Assessment

M.Soellner¹, C.Kurzahls¹, M.Rapisarda², T.Burger², S.Erker³, J.Furthner³, U.Grunert³, M.Meurer³, S.Thöler³

¹EADS Astrium Germany, Ottobrunn

²European Space Agency, The Netherlands

³German Aerospace Center, DLR

BIOGRAPHY

Matthias Soellner is navigation system engineer at EADS Astrium. He received a Ph.D. degree in physics from the Technical University of Munich. Since 2000, he works at EADS-Astrium on satellite navigation with focus on navigation end-to-end signal performance, signal design and application experiments.

Christian Kurzhals received the Dipl.-Ing. degree in electrical engineering from the Technical University of Munich in 1996. He then joined EADS Astrium, where he started in developing microwave integrated circuits for communication and scientific payloads. From 2000 to 2006 he has been with Astyx GmbH, Germany, as a principal engineer responsible for the development of distance measuring microwave sensors. Since 2006 he is again engaged with EADS Astrium as a navigation system engineer, where he focuses his work on navigation signal payload aspects.

Manuela Rapisarda is Radio Navigation engineer at ESTEC providing system support to Galileo Project Office. She received the M.S. degree (magna cum laude) in electronics engineering from the University of Catania. Since 2006 she is involved in the analysis and characterization of Navigation Satellite Payload distortions as well as in processing and performance assessment in real channel environment for present Galileo system.

Thomas Burger is Navigation Signal Engineer within the system team for the European Space Agency Galileo Project Office. His main task is the definition and implementation of the Galileo navigation signal-in-space, both within the system and towards the external world.

Dr. Burger has joined the Galileo project at ESA in 2005. From 2003 to 2005 he was working with OHB, Bremen, Germany, as SAR Performance responsible in the SAR-Lupe project, and till 2003 for 6 years in the microwave department of Astrium GmbH, Friedrichshafen, Germany, as expert for navigation systems technology and signal processing. Dr. Burger holds a Diplom-Ingenieur degree in communications engineering from the University of Karlsruhe in Germany, and a Dr.-Ing. degree in electrical engineering from the University of Darmstadt, Germany.

Stefan Erker received his diploma degree in Information Technology in 2007 from the Technical University of Kaiserslautern. He joined the Institute for Communications and Navigation at the German Aerospace Center

(DLR) in September 2007. Now he is working on the validation and signal analysis of satellite navigation systems.

Johan Furthner received his diploma in Physics from the University of Regensburg, Germany, in 1990, in 1994 his Ph.D. in Physics. In 1995 he joined the Institute of High Frequency of the German Aerospace Center (DLR), in 2000 the Institute of Communications and Navigation. He was involved in investigation and simulation of navigation satellite systems. Currently he works on the validation of the Galileo In-Orbit Validation Satellites.

Ulrich Grunert received his diploma degree of Geodesy at the Technical University of Munich (TUM), Germany, in 1999. Thenceforward he has been working in the field of satellite navigation as a scientific assistant at German Aerospace Center (DLR), Institute of Communications and Navigation. He is specialized in the topic of time transfer, time synchronization, measurement control systems and calibration.

Michael Meurer received the diploma in Electrical Engineering and the Ph.D. degree from the University of Kaiserslautern, Germany. After graduation, he joined the Research Group for Radio Communications at the TU Kaiserslautern, Germany, where he was involved in various projects in the field of communications and navigation. Since 2005 he has been an Associate Professor (PD) at the same university. Additionally, since 2006 Dr. Meurer is with the German Aerospace Centre (DLR), Institute for Communications and Navigation, where he is currently the director of the Department of Navigation.

Steffen Thöler received his diploma degree in Electrical Engineering with fields of expertise in high-frequency engineering and communications at the University of Magdeburg in 2002. Since 2002 he is working at the German Aerospace Center (DLR). Currently he works on calibration and signal analysis in the field of satellite navigation systems.

ABSTRACT

This paper deals with the offline measurement of instantaneous frequency transfer distortions and its impact to navigation performance.

Number of used signals / systems	Satellite Distortion	Receiver Distortion	User types impacted by corresponding biases
Single	All equal	Yes or no	Timing
Single	Different	Yes or no	Positioning + Timing
More than one	No	Yes	All users combining systems without receiver frequency transfer calibration
More than one	Different	Yes or no	All users without satellite and receiver frequency transfer-calibration

Table 1: Relevance of frequency transfer distortions to users

Distortions on the frequency transfer-characteristics are relevant for users mainly via reductions of usable signal power and due to biases which are difficult to be removed. For characterisation of distortion effects for real satellites and navigation receivers, several evaluation parameters are introduced, which are based on the offline processing of recorded base-band samples. Typical communication system related parameters are considered (like PSD, scatter-plot and eye-diagram) but also parameters which are derived from the correlation function shape and thus show directly the distortion-impact on navigation performance. The latter class of parameters comply correlation-loss, S-curve-bias, code-code-coherency and the frequency transfer characteristic itself.

Accurate measurements of frequency transfer distortions require careful consideration of measurement distortions. This complies at least measurement noise, sampling constraints and as most critical the calibration/equalisation of the measurement frequency transfer characteristics. For measurements with the satellite in orbit additionally care needs to be taken on multipath and interference, whereas the ionospheric dispersion reveals to be more harmless. These topics are discussed and some quantitative assessment results are given. As coarse conclusion, the reliable characterisation of satellites in orbit requires the use of high-gain-antennas (>20m diameter).

Corresponding measurement setups with BaySEF connected to the DLR measurement setup using the 30 m - Weilheim antenna of DLR GSOC in Weilheim/Lichtenau, and with the 25-m dish in Chilbolton are shown, which were used for example measurements on the GIOVE-B satellite.

Example offline signal quality assessment results for the various parameters and for the different signal transmissions in L1 from the early GIOVE-B in orbit tests (with BOC(1,1), with CBOC and with TMBOC) are presented, with the intention to test the evaluation methods rather than to assess the satellite.

The results demonstrate the absolute qualification of applied evaluation methods and will animate curious people to further assessments and analysis. For instance this concerns the conclusions, that can be drawn from certain evaluation parameter distortions.

Future improvements derived from this activity for signal quality assessment are related to small refinements on evaluation parameters and mainly on the full control over accurate measurement system characterisation and calibration.

INTRODUCTION

GNSS is facing currently very exciting evolutions. Additionally to the evolution of GPS and GLONASS, the new systems Galileo and COMPASS and regional systems like IRNSS and QZSS promise to become operational in only a few years from now. One of the most frequently asked questions is: *What is the additional use of all these systems for the user?* And one major answer is: *The user gets higher availability and reliability. Future applications may use the signals from all systems in parallel and exploit them in an intelligent way for an optimized user value.*

Indeed this is a very desirable objective, which also requests for a careful look to the interoperability issues to be solved. One issue is related to signal quality and especially to corresponding potential biases introduced within and between the different systems. Such biases result from distortions on the frequency transfer-characteristic of the satellite and/or the receiver. A basic consideration on the impact of linear and non-linear distortions on signal-biases can be found in [1,9]. Unfortunately, the systems orbit-determination and clock-synchronisation can't compensate automatically for all these bias-effects, as the receiver bias is (despite of additional receiver frequency transfer-distortions) also dependent on the receiver bandwidth and the code-discriminator in use. These parameters impact the spectral exploitation and thus the effective receiver-bias. Of course, if the receiver-bias is equal for different satellites then it is irrelevant for positioning and can be appointed to the receiver-clock offset. But as summarized in Table 1, this is not possible for a number of realistic distortion scenarios and relevant user-classes without knowing all the satellite and the receiver transfer-characteristics. For multi-system users requiring sub-nanosecond ranging accuracy this issue might become quite complex.

This system-bias and finally interoperability issue can be solved easiest just by avoiding as much as possible such relevant satellite distortions for each individual system, first.

Therefore the system design and verification of Galileo has started already from the beginning to take care of low satellite signal distortions and to allow measuring even small distortions not only on ground but also with the satellite being in orbit.

This paper is dealing with the characterisation of relevant distortions on the satellite frequency transfer. As you

might already suggest from this introduction, our focus is on the instantaneous signal quality assessment rather on the assessment of in-stabilities (like group-delay stability or code-carrier-coherency stability). We are trying to get a picture of the complete transmitted signal, whereas monitoring of in-stabilities normally evaluates changes of tracking results from navigation receivers, assuming the shape of the frequency-characteristic to remain stable.

As first, a set of evaluation parameters will be introduced which allows characterising frequency transfer distortions. Next, measurement constraints will be discussed ensuring sufficient measurement accuracy.

Example measurement setups will be presented which were used for tests on the first GIOVE test satellites.

Some example results of first successful measurements are presented, which help to obtain optimized evaluation methods for future satellite navigation frequency transfer acceptance on ground and in orbit.

Finally, a summary is given and future investigations are proposed.

EVALUATION PARAMETERS

The signal quality assessment under consideration is based on the base-band signal samples for periods of up to few seconds.

A first set of evaluation parameters is related to typical assessment parameters of communication systems, not referring too much to the navigation signal aspects.

These are [7]

- the relative envelope power spectral density estimation with Welch's periodogram method,
- the I/Q probability density after Doppler removal,
- the eye diagram, which shows the time-domain code-chip-shapes (after Doppler removal) in I- and Q, overlaid for many chips.

The Welch's method splits the time-domain signal in overlapping short parts of few microseconds, performs e.g. hamming windowing for anti-aliasing and averages the obtained power spectral densities incoherently. In order to get representative spectral envelopes, care has to be taken on two points. First, the window-length needs to be sufficient long, in order not to generate too much fold-over smoothing. The analysis of this effect is straight forward, leading e.g. to minimum window-length of 7 μ s for Galileo L1 (which includes the most narrow signal component BOC(1,1), the most sensitive Galileo signal-component for this effect) for less than 0.1 dB artefact.

Secondly, the spectral noise needs to be averaged out sufficiently well. The spectral noise is dominated by the code-noise, which is in the same order than the signal itself. It is reduced by the number of incoherent averages L according to

$$\sigma[PSD_{Welch}(f)] \approx \sqrt{\frac{1}{L}} \cdot PSD_{Envelope}(f).$$

As an example, better than 0.1 dB residual noise for Galileo-L1 (accounting for 7 μ s windows and 50% overlap) can be obtained with a signal-period of about 6.5 ms.

Comparison with the ideal spectral envelopes will allow a quite quantitative estimation of power-spectral-density deviations.

A second set of evaluation parameters relates more to the navigation aspects of the signals. They are of major relevance, as we are focusing mainly on frequency transfer distortions, which impact the navigation performance. And navigation performance is based on the correlation function. Representative for most receivers is the correlation of the incoming band-limited and down-converted signal with a binary receiver replica.

To separate from receiver distortions, this correlation is defined with respect to ideal receiver properties, especially with ideal Brickwall-type band-limitation to the bandwidth of interest.

Therefore, the correlation function is defined by:

$$CCF(\epsilon) = \frac{\int_0^{T_p} s_{BB-PreProc}(t) \cdot s_{Ref}^*(t-\epsilon) dt}{\sqrt{\left(\int_0^{T_p} |s_{BB-PreProc}(t)|^2 dt\right) \cdot \left(\int_0^{T_p} |s_{Ref}(t)|^2 dt\right)}}$$

with

- the pre-processed baseband signal $s_{BB-PreProc}$, ideally down-converted to the center-frequency of interest (e.g. E5a, E5b, E5, E6 or L1) including full Doppler removal and Brickwall-filtered to two-sided bandwidth BW,
- the reference-signal s_{Ref} , providing the ideal binary (or for CBOC four-level) base-band receiver replica signal,
- the integration period T_p , often corresponding to the primary code-period of the reference-signal under consideration.

From this normalized correlation function, the derivation of the following navigation relevant parameters is considered, which are:

- correlation loss (CL)
- code delay over early-late spacing and S-curve-bias (SCB)
- code-code coherency
- complex amplitude transfer characteristic.

Correlation-Loss

Basis of the correlation loss is the correlation power P_{CCF} , given by

$$P_{CCF}[dB] = \max_{\text{over all } \epsilon} (20 \cdot \log_{10}(|CCF(\epsilon)|)).$$

This quantifies the signal power usable within the correlation-process relative to the full available signal power. Reductions are due to relative power-share of the signal-component of interest and mismatches between incoming signal and reference-signal due to band-limitation and distortions. The distortion part $CL_{Distortion}$ is separated by comparing the correlation power with the correlation power of an ideal input signal, just Brickwall bandlimited to the bandwidth of interest

$$CL_{Distortion} [dB] = P_{CCF, Ideal s_{Input}} [dB] - P_{CCF, Real s_{Input}} [dB].$$

S-Curve-Bias:

The navigation receiver obtains the (noise-less) code-delay by the zero-crossing of the code-discriminator. To cover a major class of receivers with different spectral exploitation, here a non-coherent power discriminator is considered together with a reasonable range of early-late-spacings. The code-discriminator for early-late-spacing δ is defined by

$$SCurve(\epsilon, \delta) = \left| CCF\left(\epsilon - \frac{\delta}{2}\right) \right|^2 - \left| CCF\left(\epsilon + \frac{\delta}{2}\right) \right|^2$$

with its lock-point $\epsilon_{bias}(\delta)$ defined by

$$SCurve(\epsilon_{bias}(\delta), \delta) = 0.$$

Note, in case of more than one zero-crossing (for BOC-type signals), the delay closest to the delay of maximum correlation-power has to be selected. Then, the S-Curve-bias SCB is finally given by

$$SCB = \max_{\text{over all } \delta} (\epsilon_{bias}(\delta)) - \min_{\text{over all } \delta} (\epsilon_{bias}(\delta)),$$

considering all δ in the range $[0, \delta_{max}]$, with

$$\delta_{max} [\text{chips}] = \begin{cases} \frac{1.5}{4 \frac{m}{n} - 1} & \text{for a BOC}(m,n) \text{ reference Signal} \\ 1.5 & \text{for a BPSK } n \text{ reference Signal} \end{cases}$$

Note, for CBOC the BOC(6,1) component is relevant for δ_{max} . Of course different discriminators might provide slightly different biases, but above definition of bias-spreading is expected to be quite representative from a system point of view. This is because it is based on a typical discriminator and as the wide-range of early-late-spacing corresponds to a wide range of different spectral exploitations of the input-signal.

Code-code coherency:

The code-code coherency quantifies the difference in the delay of the correlation maximum for different signal components of a commonly transmitted navigation signal. This relative evaluation requests for the same input signal period and all reference signals to be equally synchronized.

Complex amplitude transfer characteristic:

For a linear system, the complex transfer characteristic $H(f)$ is given by the spectrum of the output-signal divided by the spectrum of the input-signal. With non-linearity included within the system (as usually the case for navigation satellites), spectral contributions of signal to the q^{th} power are added (with several integer and non-inter q). This provides noise-like contributions, preventing successful transfer-characterisation with above definition. But

when concentrating on the useful correlation power and averaging over small spectral regions, a relevant transfer-characteristic estimation can be obtained by

$$H(f) \cong \frac{\int H_{Average}(f') \cdot CCF_{Real}(f - f') df'}{\int H_{Average}(f') \cdot CCF_{Ideal}(f - f') df'}$$

with

- $CCF(f)$ the spectrum of $CCF(\epsilon)$
- $H_{Average}(f)$ a moving average filter with a bandwidth much lower than the smallest chip-rate.

GENERAL MEASUREMENT REQUIREMENTS

To characterize the distortions on the transmitted signal, above parameters shall be evaluated from sampled base-band signals. The measurement itself needs to avoid additional distortions. Most critical aspects on that are discussed in this chapter.

For measurements with the satellite on ground, major measurement distortions are expected from thermal noise, measurement equipment frequency transfer distortions uncertainty, sampling rate and quantisation. Further sources like clock-phase-noise are usually small for high quality oscillators.

For measurements with the satellite in orbit, additional distortions of inband-interference and multipath are most dangerous. Also the ionospheric dispersion needs to be considered. All these effects are discussed in the following, providing also some analytic and numeric results of corresponding error analysis.

Sample-rate:

The analysis is limited to the complex base-band signal of a certain two-sided bandwidth BW. Therefore, the signal needs to be bandlimited slightly broader, before sampled with at least corresponding Nyquist rate. Thus typically a sampling rate of about 1.2 x BW is sufficient. Nevertheless, small code-delay artefacts (in the order of 10 picoseconds) might be obtained with such minimum sample-rates, due to deviations of the sampled signal from full periodicity.

Parameter evaluation has to be performed with the bandlimited signal to be upsampled to much higher rates, in the order of 1 GHz. Such high rates are required for appropriate code-delay resolution of much below 0.1 ns and to a minor importance also for correlation-loss resolution of below 0.01 dB.

Sampling-Quantisation:

As long as sampling is performed asynchronous to the input-signal periodicities and it is ensured that the signal is not clipped, the impact of quantisation is mainly limited to noise. Corresponding effect can be well estimated by the signal to quantisation noise ratio (SQNR), given for a sinusoidal signal and full range quantisation to n -bits by the well known equation [e.g. 6]

$$SQNR[dB] = 1.76 + 6.02 \cdot n.$$

Note, this contribution might become relevant for high-gain-antennas and low number of quantisation-levels accounting also for the exploited range.

Thermal-noise:

For correlation-loss evaluation, the input signal-power is assumed to be much above the noise-floor and thermal noise is neglected normally. But this is often not appropriate. Already for SNR < 16 dB, (which correspond to C/N=93 dBHz for 40 MHz noise-bandwidth), the correlation-loss gets an offset of 0.1 dB. Only when knowing the SNR accurately, this error can be compensated.

Thermal noise is also relevant for code-delay evaluations. Analysis showed a worst case SCB jitter of all Galileo signals of about 60 ps for SNR = 70 dB (for BOC(1,1)). To reduce the jitter below 5 ps for a C/N = 90 dBHz, this requires about 1.5 s averaging.

Measurement equipment distortion uncertainty:

The transfer-characteristic of the measurement equipment of course impacts the evaluation results and therefore needs to be taken into account. Most appropriate is the measurement of corresponding transfer-characteristic with a certain calibration method (e.g. with appropriate NWA-measurement) and applying the inverse inband characteristic during pre-processing of the base-band samples. Nevertheless a certain uncertainty remains. The question is how much residual amplitude and phase-distortion is allowed. For phase-distortions alone, mainly its group-delay characteristic is relevant. Simulations have shown that at maximum the SCB-contribution is about half the peak-to-peak residual group-delay variation. Amplitude distortions alone are just relevant for CL-evaluation. Then, the correlation-loss error corresponds at maximum to the peak-to-peak amplitude uncertainty. Up to now, the authors don't know any rigorous analysis about the impact of combined amplitude and phase-distortion uncertainties to CL and SCB accuracy.

Multipath:

Static multipath is mainly relevant for code-delay and finally SCB evaluation. An estimation of its relevance can be obtained already by considering the well known multipath-envelopes for low reflection-power. As an example, the BOC(1,1) multipath envelopes for -60 dB reflection power and several early-late-spacings and non-coherent power-discriminator are shown in Figure 1. Contributions of such order are still relevant, demonstrating that multipath needs to be avoided as much as possible with strong antenna side-lobe suppression.

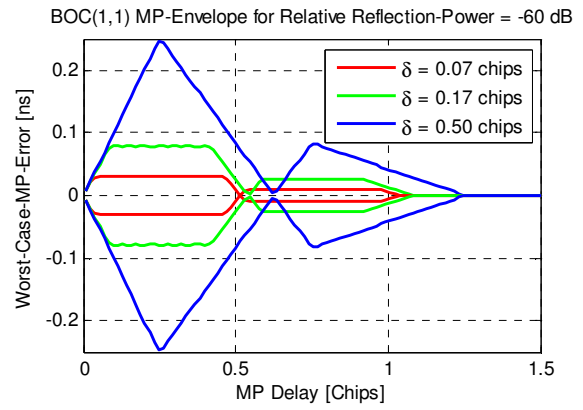


Figure 1: Impact of low multipath on code-delay

Interference:

Analysis has shown that inband spurious distortions may become relevant, if its frequency complies with the strongest spectral signal lines and if applied with 90° phase-offset. In this worst-case, up to few 100 ps distortions on the SCB can be obtained for only -30 dB spurious/interference power relative to the total signal power. Therefore, a rigorous signal quality assessment would request for simultaneous interference detection and assessment.

Ionospheric dispersion:

The ionospheric dispersion relative to the center-frequency f_0 can be described by the phase-distortion of [4]

$$\varphi(f) = -2\pi \cdot f \cdot \frac{40.3 \cdot TEC}{c \cdot f_0^2} \cdot \left(1 - \frac{f_0}{f}\right)^2,$$

with the speed of light c and the total electronic content TEC [m/s²]. The corresponding group-delay distortion is given by

$$\begin{aligned} GD(f) &= -\frac{1}{2 \cdot \pi} \cdot \frac{d\varphi}{df} = \frac{40.3 \cdot TEC}{c \cdot f_0^2} \cdot \left(1 - \left(\frac{f_0}{f}\right)^2\right) \\ &\cong \frac{40.3 \cdot TEC}{c \cdot f_0^3} \cdot df \cdot \left(2 - 3 \cdot \frac{df}{f_0}\right) \end{aligned}$$

with the frequency offset df from the center-frequency.

For L1, as example, this results in an almost linear GD variation with peak-to-peak change over +/- 20 MHz of 53 ps per TECU (1 TECU = 10¹⁶ m/s²). But the code delay variation is just impacted by a small part of that value. Simulations resulted in about 1% of the peak-to-peak value for BOC(1,1) and even much less for BOCc(15,2.5). More relevant impacts of the ionospheric dispersion might be obtained for the E5 signal when considered as broadband AltBOC signal.

As general conclusion from above discussion it can be concluded, that corresponding signal quality analysis require the use of high gain antennas with diameters in the order of 20 – 30 m as for the Weilheim deep-space antenna or the Chilbolton observatory. This is not only to lift the signal out of thermal noise but even more in order to suppress interference and multipath from the environment.

WEILHEIM MEASUREMENT SETUP WITH BAYSEF

For testing the evaluation of signal quality parameters, one rack of the BayNavTech™ Signal Experimentation Facility (BaySEF) was installed in a co-operation between EADS Astrium and DLR to the 30 m dish of DLR-GSOC in Weilheim/Lichtenau.

The dish, shown in Figure 2, is a typical Cassegrain antenna with the eponymous signal path shown in Figure 3. Foremost the signal is reflected from a parabolic reflector to the hyperbolic-subreflector. With the help of another sub-reflector it is then directed to the cabin where the signal is received using a newly developed circular-polarized Quad-ridged waveguide feed, see Figure 4. More details about the antenna setup can be found in [8].

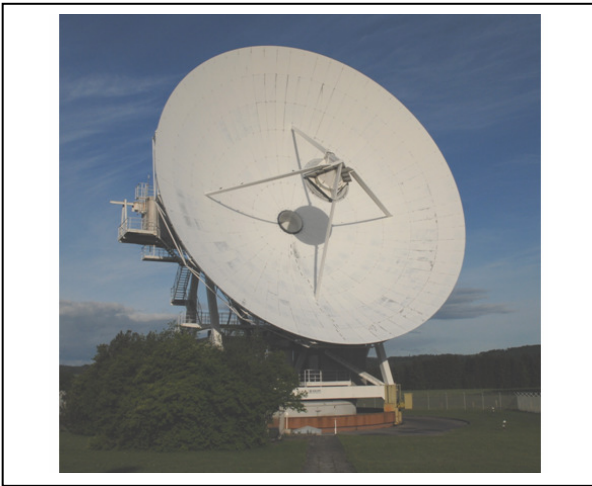


Figure 2: 30 m dish of DLR in Weilheim/Lichtenau

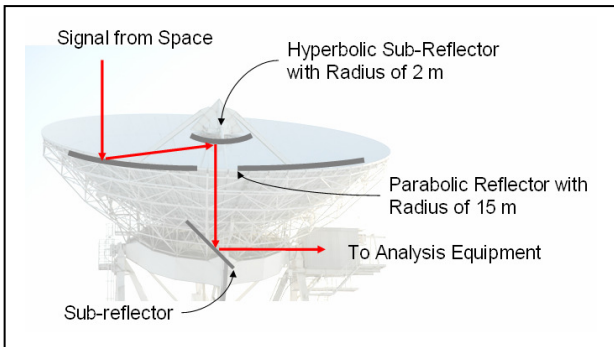


Figure 3: 30 m dish, schematic diagram with signal path.



Figure 4: Quad-ridged waveguide feeder

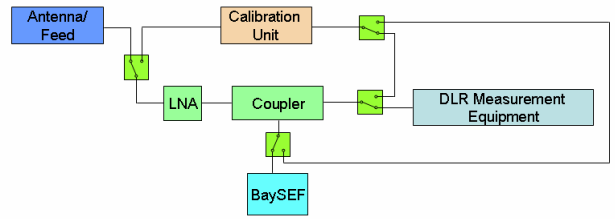


Figure 5: Blockdiagram of Weilheim measurement setup for signal quality and EIRP measurements

The overall measurement setup, with the block-diagram shown in Figure 5, was not only for signal quality analysis of the satellites frequency transfer-characteristics but mainly also used for DLR’s absolute signal power / EIRP measurements. Therefore major parts of the setup are for calibration tasks. To achieve the required accuracy an extensive work with determination of the absolute antenna gain, the antenna pointing and the transfer function of the whole measurement system had to be done. Each of these measurements was performed continuously by DLR and EADS using at least two different methods to get reliable results and validate the used measurement methods. The signal quality results shown in this paper are derived from signals, acquired and recorded with one of two available BaySEF racks, a picture of which is shown in Figure 6.

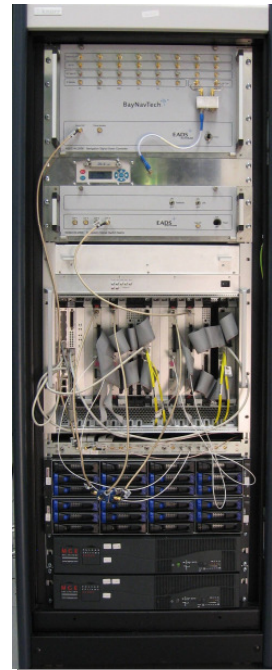


Figure 6: Single BaySEF measurement system

The BaySEF can be characterised as a flexible wideband GNSS receiver and signal performance evaluation platform for reception and processing of navigation signals. Main applications are the verification and monitoring of GNSS SIS and the support for application design. Key features most relevant for the signal-quality assessment of this paper are:

- Simultaneous processing & synchronized recording of up to 4 navigation frequency bands,
- RF 3-dB-bandwidth of more than 100 MHz in E5 and more than 50 MHz in all other bands (E5a, E5b, L2, E6, L1),
- Maximum recording capacity of 120 MByte/s per frequency band,
- Flexible decimation and quantisation,
- Recording capacity of more than 80 minutes per frequency band,
- Remote control of data-acquisition.

To get a more comprehensive overview on all the BaySEF capabilities, the interested reader is referred to [2, 3].

As discussed already in the last chapter, the calibration of the measurement systems transfer-characteristic is of utmost importance.

It has been split in two parts: The RF-equipment from feed until BaySEF is measured with an integrated NWA. The BaySEF characteristic itself is measured offline with the help of a navigation signal generator relative to a vector signal analyser (FSQ from R&S). This calibration measurement was repeated at an interval of more than two month, which provided only small differences as shown in Figure 7 for L1, with less than 0.2 dB peak-to-peak amplitude changes, less than 1 deg phase changes and less than 2 ns changes in the group-delay characteristic within 40 MHz.

The product of measured RF-equipment and BaySEF transfer characteristics was used to derive the equalisation filter applied in post-processing to the recorded samples, providing a quite reliable measurement system calibration in amplitude and phase.

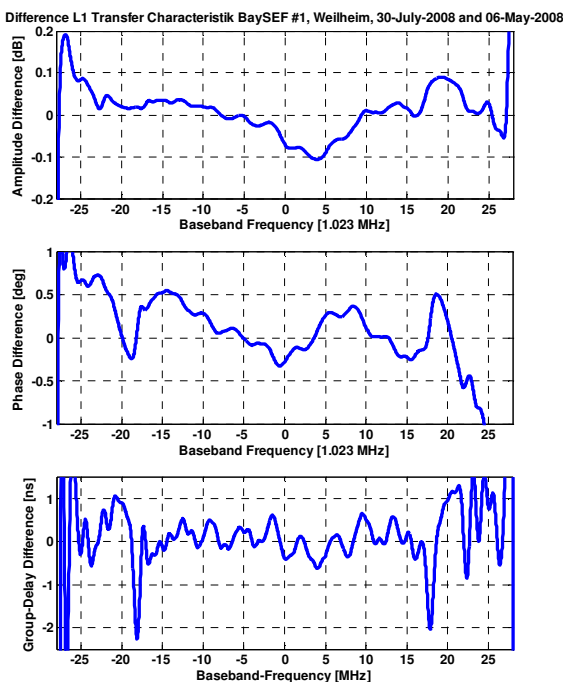


Figure 7: BaySEF transfer-changes in a 85 days interval

CHILBOLTON MEASUREMENT SETUP

The highly directive and fully steerable parabolic antenna of the Rutherford Appleton Laboratory (RAL) Chilbolton Observatory (UK) -with its 25-meters dish- is suitable for the signal quality analysis deal with in this paper.

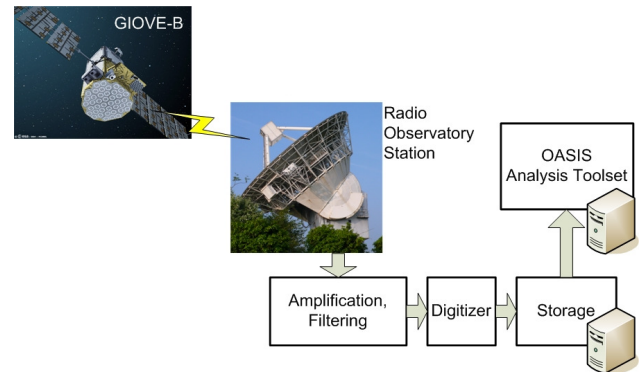


Figure 8: Blockdiagram of Chilbolton measurement setup

The Chilbolton measurement set up is described in the block-diagram in Figure 8. Once the signal from space is acquired by the antenna, it undergoes to amplification and filtering stages before being down-converted and digitized by the Agilent Power Spectrum Analyzer (PSA) E4440A with option 122 (i.e. including wide bandwidth digitizer) whose most relevant features for the signal-quality assessment of this paper are:

- Maximum sampling frequency of 102.4 MHz
- Maximum useful bandwidth of 80 MHz
- Maximum recording capacity of 128 Msamples per signal

The digitizer is disciplined by the external master frequency reference HP 58503B.

Since the Offline signal quality assessment can be derived from measured signal periods of up to few seconds length the storage consist of a simply external PC connected by mean of the LAN to the PSA.

EVALUATION EXAMPLES

In this chapter, GIOVE-B example results for the different evaluation parameters are shown, which were obtained from measurement data obtained either in Chilbolton or Weilheim.

As first, in Figure 9, an example power-spectral density envelope is shown, derived with Welch's method from few milliseconds of signal-samples measured in Chilbolton at 07.05.2008. The overlay with the ideal baseband spectral envelope (accounting also for corresponding interplex product-signals) allows identifying signal components of $\text{BOC}_c(15,2.5)$ and MBOC as part of the signal. This comparison also reveals a clear asymmetry between the $\text{BOC}_c(15,2.5)$ lobes in the order of at least 1 dB, which is already widely recognized.

But how far this is relevant for navigation performance is not clear from the spectrum alone.

It is worthwhile to mention, that the spectrum also don't tell us the MBOC-type, i.e. if CBOC or TMBOC is transmitted.

At least this latter differentiation can be performed from the I/Q-sample probability distribution. Such scatter plots are shown in Figure 10 from Weilheim measurements of CBOC (09.05.2008) and TMBOC (29.05.2008) signals, derived from about 50 ms signal-samples. Note, for this and all following evaluations, the signal-samples had to be Doppler-compensated first.

The lower plot can be clearly identified as the interleaved CBOC signal, whereas the upper plot applies to the interleaved TMBOC (but would also apply to BOC(1,1) interleaved). The ideal baseband infinite bandwidth signals are constant envelope with eight and six phase-states, respectively. Due to band-limitation, distortions and noise-jitter, the individual phase-states have been blown up, and transition traces become visible. Also the symmetry of phase-states becomes slightly deformed. Again also for this parameter it is not directly obvious how it relates to measurable navigation performance. This is also the case for the eye-diagrams.

But before, a general statement: For all following evaluation results the L1 signals have been Brickwall band-limited to 40.92 MHz (= 40 x 1.023 MHz), which was the performance bandwidth of interest, and upsampled to rates of 720x1.023 MHz (Chilbolton) or 575 MHz (Weilheim), respectively.

For the eye-diagrams, several periods of 1 MHz code-chips have been overlaid for different GIOVE-B signals

measured in Chilbolton, and I- and Q-components are shown separately. Here now a clear separation between all the options of L1 pulse-shapes CBOC, TMBOC and BOC(1,1) is possible. For CBOC, the small BOC(6,1) amplitude pulse-shape modulation is visible, whereas in TMBOC, few pure BOC(6,1) code-chips are inserted between the conventional BOC(1,1) code-chips. In the Q-component, the strongly-bandlimited BOCc(15,2.5) pulse-shape is visible but also the product signal is included, with small parts of other pulse-shapes. The deviation from ideal expectation and the variation has several reasons. This comprises noise, band-limitation, I-Q cross-coupling due to non-linear distortions etc. Relevant for differences in succeeding code-chip-shapes is also the memory of preceding code-chips via the filter impulse response. Within communication, the opening of the 'eyes' can be related to bit-error performance quite directly. It would be probably worth to investigate this relation also concerning navigation-performance, which might also be linked. But finally, navigation is based on the correlation-function evaluation, providing a more integrated signal evaluation, also with stronger impact of the chip-transitions.

Therefore, as an example, the GIOVE-B correlation function shapes of the CBOC-data and pilot-signals are shown in Figure 12, and from BOCc(15,2.5) in Figure 13, all derived from Weilheim measurement data from 09.05.2008. Here, the shapes are averaged over several code-periods (about 0.5 seconds).

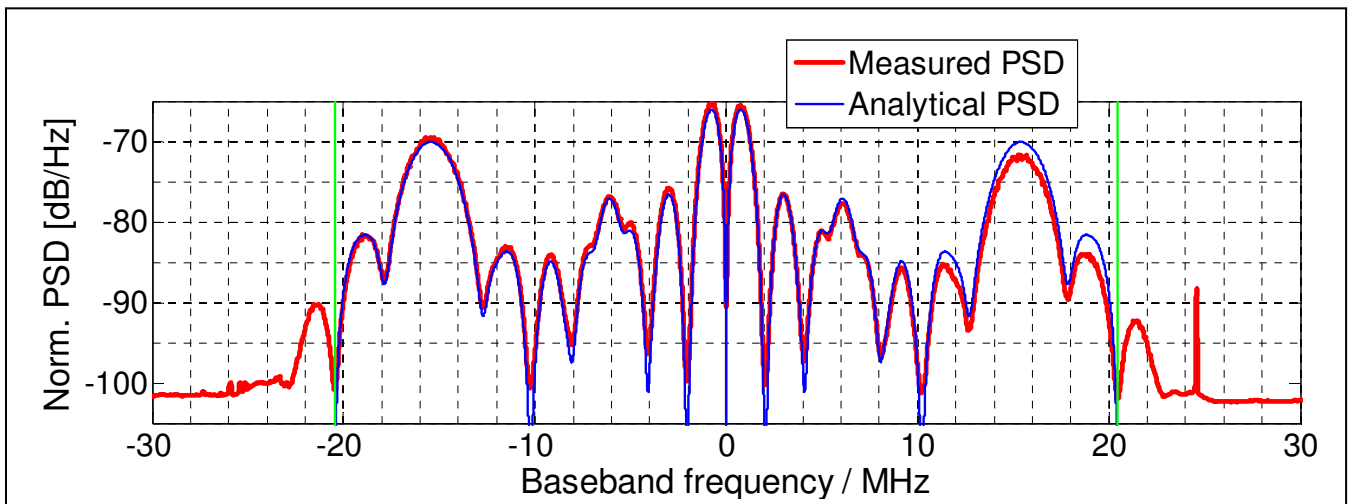


Figure 9: PSD of GIOVE-B L1 CBOC-signal

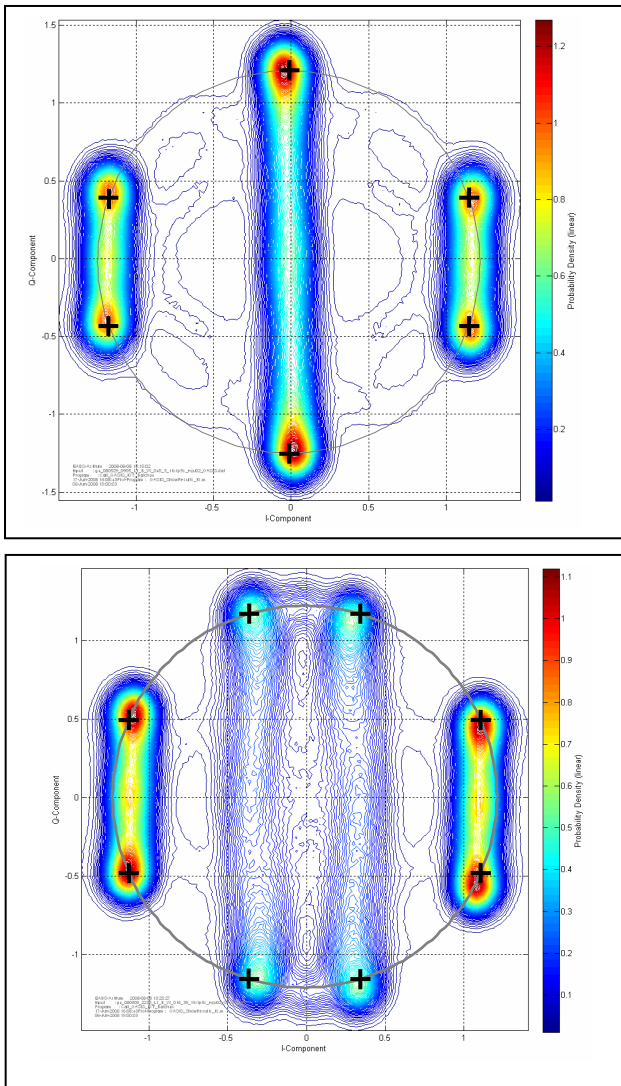


Figure 10: Scatter-plots of GIOVE-B L1-TMBOC (upper plot) and L1-CBOC (lower plot), together with black crosses at ideal base-band signal phase-states.

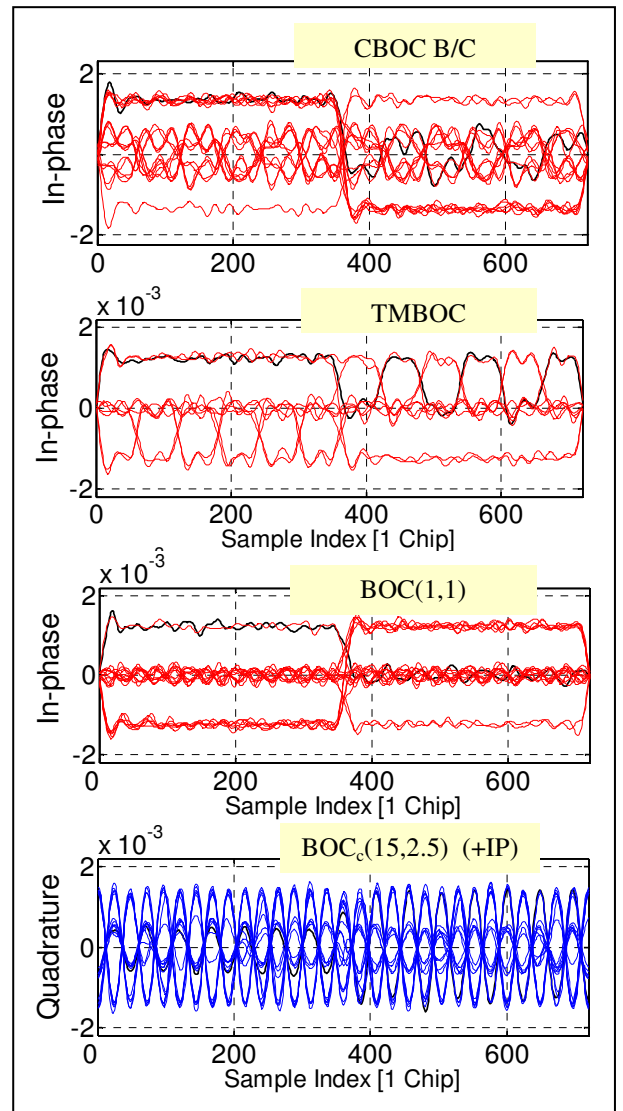


Figure 11: Eye-diagrams of GIOVE-B L1-CBOC, TMBOC, BOC(1,1) and BOCc(15,2.5) + Prod.-signal

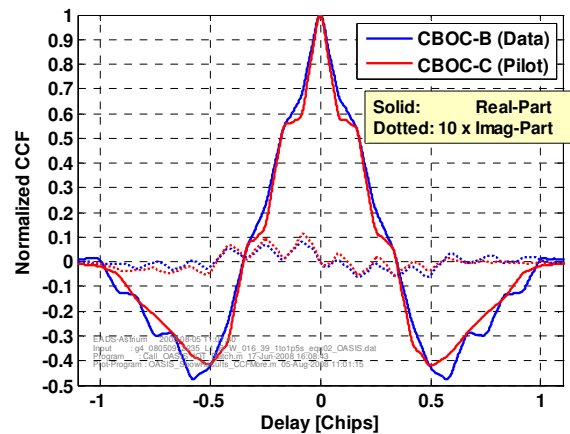


Figure 12: GIOVE-B L1-CBOC correlation function shape.

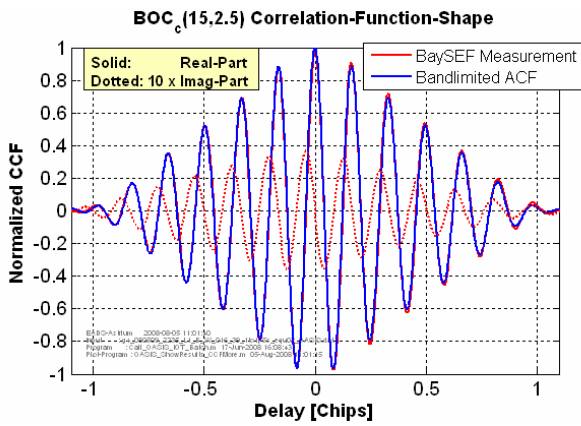


Figure 13: GIOVE-B L1-BOCc(15,2.5) correlation function shape

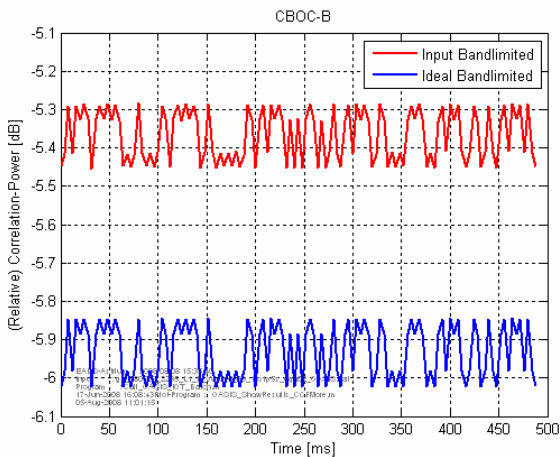


Figure 14: GIOVE-B example correlation-power evaluation result for CBOC-B.

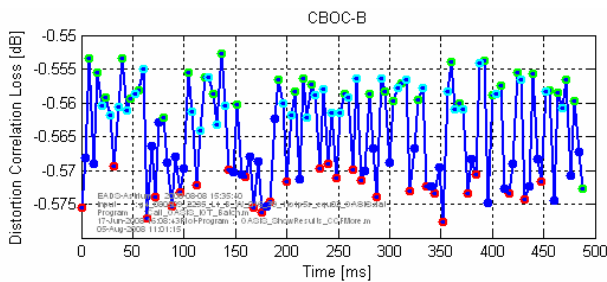


Figure 15: GIOVE-B example distortion correlation-loss evaluation result for CBOC-B.

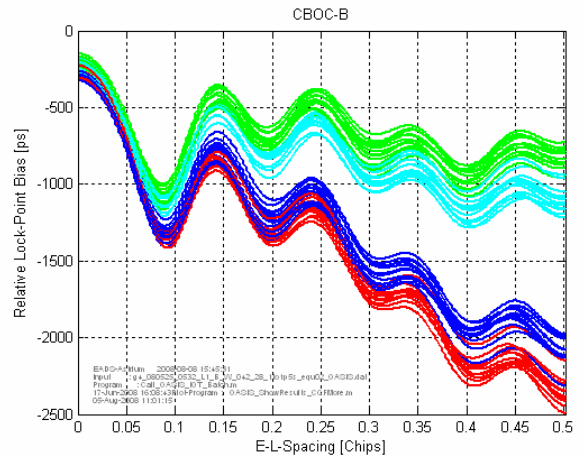


Figure 16: Lock-point-bias in dependency of early-late-spacing for GIOVE-B BOC(1,1) example

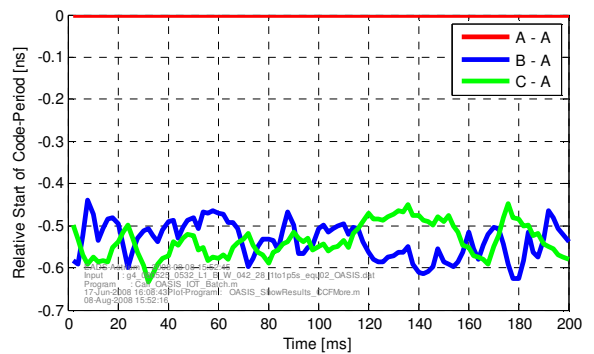


Figure 17: GIOVE-B L1 with BOC(1,1) example code-code-coherency result

The differences in shapes are not due to distortions but due to different sign of BOC(6,1) sub-carrier in B- and C-channel. A direct visibility assessment of these shapes offer not too much conclusions, despite of its imaginary-parts, which should not be but are due to signal distortions. Note, the imaginary part is here already 10 times amplified in order to stress its presence. But how far is this relevant ?

For the shape of the BOCc(15,2.5) correlation-function also a small asymmetry in the real-part is visible when comparing to the ideal band-limited auto-correlation-function. This signal distortion effect is clearly relevant leading to increased false lock probability in acquisition and tracking, which is the first clear aspect of identified relevance for navigation performance.

In order to find more quantitative aspects, the finally relevant performance parameters of correlation-loss and bias-behaviour are evaluated from the correlation-function shapes.

Example results on the correlation power evaluation for GIOVE-B CBOC-B are shown in Figure 14, with the red curve showing the correlation-power of succeeding code-periods, relative to the total signal (which includes also the CBOC-C, and BOCc(15,2.5) signal components). What seems to be surprising is the strong 'jitter' of more than 0.1 dB. But when analysing also an ideal reconstruction of the multiplexed baseband-signal (also

exactly synchronized to the input-signal), shown as the blue curve in Figure 14, almost the same jitter is obtained. In fact it turned out, that the GIOVE-B code-cross correlations between B- and C-component are mainly responsible for that, which can have four different values. The difference between correlation-power of the band-limited input-signal and of the band-limited ideal reconstruction signal is finally the distortion correlation-loss, which is shown in Figure 15.

This distortion correlation-loss here is negative, which means we have not a loss but a gain relative to the undistorted case. How is this possible ? It is because the distortion obviously results mainly in a power redistribution of the signal-components relative to each other. The wide-band signal-component $\text{BOC}_c(15,2.5)$ is stronger band-limited (by the distortion), relative to the narrow-band CBOC-signal component, which effectively gains relative power by this.

The variation in distortion correlation loss after compensating for the code-cross-correlation effects by above described analysis is in the order of 0.02 dB. But this is still much more than expected for the given noise-level. The reason for that is the residual interaction between distortions and code-cross-correlations. This becomes apparent from the colored dots in Figure 15, where equally colored dots correspond to periods of equal code-cross-correlation.

As next, we consider the bias of NCELP-discriminator lock-point in dependency of early-late-spacing as derived from the correlation-function shapes. An example result for measured GIOVE-B L1 signal transmission with $\text{BOC}(1,1)$ and evaluated for the $\text{BOC}(1,1)$ B-component is shown in Figure 16 evaluated for 125 succeeding code-periods. Again as for correlation-loss analysis, different colors correspond to different code-cross-correlation contributions. As relevant code-cross-correlation mainly affects the asymmetric contribution for 1 code-chip delay, its impact on the discriminator lock-point bias increases with increasing early-late-spacing. Variations between the curves of equal colors are due to residual thermal noise. Thus representative results require further averaging over many code-periods, even when evaluated from high gain antenna measurements. For finally user-representative bias-values, an adequate averaging over the different relevant code-cross-correlation cases needs to be performed. And as also typical for the bias seen by a certain user-receiver, the results don't reflect only the satellite distortions but also receiver contributions. In fact, the order of measurement system calibration uncertainty and instability for these results (see e.g. Figure 7) is expected to provide here still relevant contributions. Accurate measurement system calibration is therefore one of the most critical issues for exact signal quality assessment of satellite transfer characteristics and its impact on navigation performance.

The same applies for the example results on code-code coherency, shown in Figure 17 for the GIOVE-B L1-transmission with $\text{BOC}(1,1)$. Generally, such a de-coherency between signal-components is not unexpected due to group-delay ears of analogue filters close to the

transition range, which in this case result in higher delays for the wide-band $\text{BOC}_c(15,2.5)$ (A-) component than for the narrow-band (B- and C) components of $\text{BOC}(1,1)$.

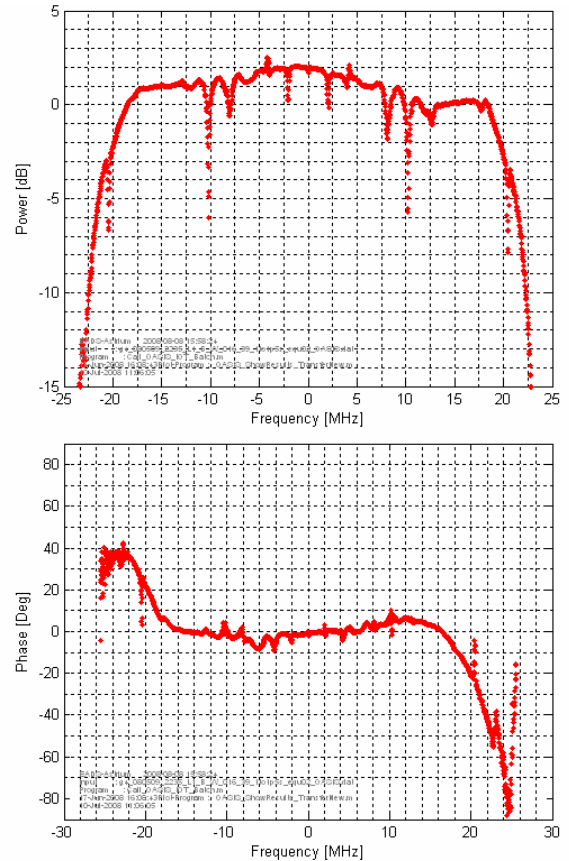


Figure 18: GIOVE-B L1 with CBOC example amplitude and phase frequency transfer characteristic results.

This leads us to the last example of evaluation parameters shown in Figure 18, which is the transfer-characteristic derived from a measurement of GIOVE-B L1 with CBOC-transmission (here without applying the Brickwall band-limitation). The transfer-characteristic has a frequency resolution of 25 kHz and is obtained by averaging over more than 50 ms for noise suppression. Despite of residual measurement-equipment contributions, such transfer-characteristics of course have artefacts at the spectral zero-crossings of the signal itself. But further discontinuities are also due to the satellite amplifier which is operated for power efficiency reasons close to its saturation and thus contributes considerable nonlinear distortions.

Here we come back to the problem, that also the evaluation-parameter of the transfer-function does not allow a direct conclusion on its navigation performance impact. Nevertheless it is a very important parameter, as it can be used in a very effective way for further analysis. Just the application of a single filter with corresponding transfer-function to the ideal signal will provide the full correlation-function distortions as obtained by several interrelated linear and non-linear distortions of the end-to-end signal transmission and reception process. In case all the satellites of the different navigation systems finally can't avoid user dependent biases to occur, it is this

characteristic which is required for optimum user related bias analysis and elimination.

CONCLUSION AND FUTURE WORK

Signal quality assessment as discussed in this paper is to identify stable distortions on the end-to-end frequency transfer-characteristic and its impact to users, mainly in form of correlation-power losses and biases.

Basing on recorded base-band signal samples, several evaluation parameters were introduced and discussed, comprising PSD-envelope, scatter-plot, eye-diagram and the correlation based evaluation parameters of correlation loss, S-curve-bias, code-code-coherency and the extraction of complex transfer-characteristic also for non-linear systems.

The measurements for transfer-characteristic distortion assessments require careful control over potential measurement distortions. Whereas thermal noise can be reduced 'just' by longer averaging periods, calibration uncertainty (including stability) of the measurement equipment transfer function is probably most critical. For in orbit satellite characterisations, also multipath gathered via antenna side-lobes and interferences have to be avoided, leading overall to the strong recommendation for using high gain antennas for such measurements.

Corresponding measurement systems at Chilbolton and with BaySEF at Weilheim were used to acquire samples of GIOVE-B early signal transmissions in L1 including the BOC(1,1), CBOC and TBOC signal options.

The offline signal quality assessment results demonstrate very successful parameter evaluations, leading for several parameters to further questions of quantitative links between signal-distortion and evaluation parameter distortions. Even the problematic effects of varying code-cross-correlation could be extracted and partly already compensated (for correlation-loss-evaluation). As a refinement for user-representative S-curve bias evaluation, an adequate averaging over code-cross-correlation effects is planned to be added in future.

Finally, also the successful evaluation of frequency-transfer-characteristics of the non-linear system with high frequency resolution is demonstrated. Generally, this is the key for optimum user related bias elimination. Further analysis is required to identify about the full range of information and its accuracy that can be derived from such evaluations.

The offline signal quality assessment methods shown in this paper demonstrated already high maturity. Therefore, in order to reach accurate satellite transfer characterisations, the focus needs to be directed towards accurate measurement system characterisation. Main aspects are to have a measurement system with known negligible non-linearities, reference measurement devices or calibration sources with low and known uncertainty and to control also the stability of the measurement system transfer accurately.

With successful completion of these tasks, signal quality assessment of the demonstrated kind can become a crucial tool helping to avoid inter- and intra-system biases to a very low level for a wide range of users.

ACKNOWLEDGEMENTS

BaySEF is part of BayNavTech™ program, which is supported by the Bavarian Government (Ministry for Economic Affairs, Infrastructure, Transport and Technology). The measurements in Weilheim have been performed in the frame of a cooperation between EADS-Astrium and DLR.

REFERENCES

- [1] M. Soellner, et al, 'The impact of linear and non-linear signal distortions on Galileo code tracking accuracy', ION-GNSS 2002, Portland, Oregon
- [2] M. Soellner, et al, 'The BayNavTech™ Signal Experimentation Facility (BaySEF™) is ready for assessing GNSS signal performance', ION-GNSS 2007, Fort-Worth, Texas
- [3] M. Kaindl, M. Soellner, C. Zecha, R.Kohl, 'Performance analysis of Giove-A signals in comparison with GPS based on wideband measurements with the BayNavTech™ Signal Evaluation Facility (BaySEF™)', ION-GNSS 2007, Fort-Worth, Texas
- [4] Hargreaves, J. K., The solar-terrestrial environment, Cambridge University Press, 1992.
- [5] G.Perello, M.Malik, M.Falcone, Selected RNSS Measurements and Analysis, ENC-GNSS-2008, Toulouse
- [6] J.G.Proakis, D.G.Manolakis, *Digital Signal Processing*, Prentice-Hall
- [7] Another candidate parameter would be the received signal power or translated to the satellite the equivalent isotropic radiated power (EIRP). But as it does not provide contributions to the frequency transfer characterisation, it is not considered here. For details on EIRP characterisations refer to [5].
- [8] Montenbruck, Oliver; Günther, Christoph; Graf, Sebastian; Garcia-Fernandez, Miquel; Furthner, Johann; Kuhlen, Hanspeter (2006): GIOVE-A Initial Signal Analysis. GPS Solutions, 1ß (2), Springer, S. 146 – 153
- [9] Graf, Sebastian; Günther, Christoph (2006): *Analysis of GIOVE-A L1-Signals* In: Proc. ION GNSS 2006, S. 1560 - 1566, ION GNSS, Fort Worth, Texas (USA)

ABBREVIATIONS

BaySEF	BayNavTech™ Signal Experimentation Facility
CL	Correlation Loss
HGA	High Gain Antenna
NCELP	Non-Coherent Early-Late Power Discriminator
ns	nano-second
ps	pico-second
PSD	Power Spectral Density
SCB	S-Curve-Bias
SNR	Signal to Noise Ratio